5.2 TELESCOPING MODEL APPROACHES TO EVALUATE SEVERE CONVECTIVE STORMS UNDER FUTURE CLIMATES

Robert J. Trapp, Brooke A. Halvorson, and Noah S. Diffenbaugh
Department of Earth and Atmospheric Sciences
Purdue University
West Lafayette, IN 47906

1. INTRODUCTION

A consistent result in climate model projections of future anthropogenic climate change is that the frequency of extremes in annual, seasonal, and daily precipitation will increase, particularly over North America (IPCC 2001, and references therein). Because the climate dynamics governing the transmission of global-scale changes in radiative forcing to local-scales are not well understood, it has not yet been established whether and/or how the projected extreme precipitation will be manifest as locally intense, convective precipitating storms with several-hour time scales. This is the ultimate goal of the research presented herein.

The organization of cumulus clouds into intense convective precipitating storms is governed primarily by larger-scale or ambient distributions of temperature, moisture, and winds. One therefore could use global (and regional) climate model simulations to make physical arguments on how convective storms might be affected by the ambient distributions of temperature, etc., under future climates.

Brooks (2006) has begun such an effort for the current climate, using the National Center for Environmental Prediction (NCEP) and National Center for Atmospheric Research (NCAR) Reanalysis Project (NNRP) global dataset. For completeness, and following the methodology of Brooks (2006), we are, in a separate study, pursuing this using the simulations of current and future United States regional climate presented by Diffenbaugh et al. (2005).

However, we recognize that arguments based this *indirect* approach will be limited, since they must make the tenuous assumptions that (i) convective storms have or will initiate in these environments, and also that (ii) the complex scale interactions between the storms and their local environments (such as those involving mesoscale convective vortices) are negligible.

We avoid these assumptions in the following *direct* approach by explicitly simulating convective storms. As described next, we follow telescoping modeling approaches that culminate in 3D, convection-permitting model simulations. Figure 1 illustrates the basic concept.

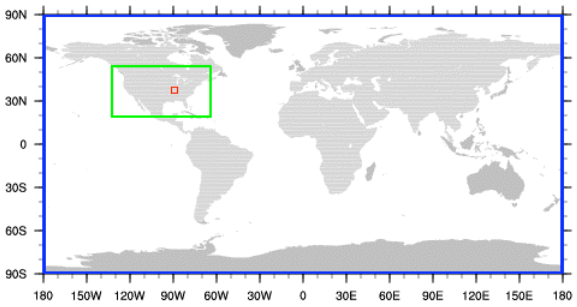

FIG 1. Schematic of a telescoping modeling approach using a global climate model (domain in blue outline), a regional (climate) model (domain in green outline), and a cloud-resolving or convection-permitting model (domain in red outline).

Given a number of possible ways to implement this concept, the objective of the current

[1] *Corresponding author*: Robert J. Trapp, Department of Earth and Atmospheric Sciences, Purdue University, 550 Stadium Mall Drive, West Lafayette, IN 47906. Email: jtrapp@purdue.edu

study is to determine the telescoping model strategy that is most accurate in terms of the antecedent conditions on the synoptic and mesoscale, the initiation of deep convection, the mode of the convective storms, and the representation of severe weather associated with these storms. Two specific strategies, the Regional Climate Modeling Approach (RCMA) and the Weather Forecasting Approach (WFA), are identified and evaluated based on simulations of historical convective storm events.

2. TELESCOPING MODELING

a. The components

The basic components of the telescoping modeling technique are a global climate model or global dataset, a regional model, and a convection-permitting model.

(1) Global data

Global data from the National Center for Environmental Prediction (NCEP) and National Center for Atmospheric Research (NCAR) Reanalysis 1 Project (NNRP) (Kalnay et al. 1996) currently serve as the primary source of model boundary and initialization information in both modeling approaches. NNRP data are available from 1948 to current day on a 2.5 × 2.5 degree latitude/longitude grid (~210 km horizontal gridpoint spacing) at 6-h intervals.

Though not shown here, we have also successfully implemented a global climate model in the telescoping model technique. The model data have been generated thus far with the NCAR Community Atmospheric Model (CAM) forced with observed sea-surface temperatures.

(2) Regional model

The regional model need not necessarily be a regional *climate* model, but for the RCMA we utilize the Abdus Salam Institute for Theoretical Physics Regional Climate Model, version 3 (RegCM3). Based on earlier versions of RegCM developed at NCAR – and originally on the NCAR-Pennsylvania State University mesoscale model, version 4 – RegCM3 is a hydrostatic, compressible, finite difference model that uses vertical sigma coordinates (e.g. Giorgi et al. 1993; Giorgi and Mearns 1999; Pal et al. 2000).

For the current study, RegCM3 is applied to a domain centered at 37.581ºN, -95ºW (Fig. 4). The horizontal grid consists of 126 (78) points in longitude (latitude), with a 55.6-km gridpoint spacing; the vertical grid has 18 sigma levels. Given the NNRP data as initial and boundary conditions, the model is continuously integrated in time for more than one year prior to each event. Specifically, the time integrations are: 1 January 1973 – 5 April 1974, and 1 January 2000 – 10 May 2001. Other details such as the various model parameterizations are given in Table 1.

Table 1. RegCM3 model physics parameterization schemes.

Parameterization	**Name**
Radiation Scheme	NCAR CCM3 radiation scheme
Land Surface Model	BATS1E (Biosphere-Atmosphere Transfer Scheme)
Planetary Boundary Layer	Non-local diffusion scheme
Convective Clouds and Precipitation	Grell Scheme

(3) Convection-permitting model

The "advanced research" version of the Weather Research and Forecasting (WRF) model Version 2.1.2, a fully compressible, non-hydrostatic model (Michalakes et al. 2001; Skamarock et al. 2005), is used here both as regional or traditional mesoscale

model and a convection-permitting model. This is permitted through the WRF model's fully interactive grid-nesting capabilities. Table 2 provides specific details of our application of the WRF model in the WFA as well as the RCMA.

Relevant to the current study are the recent experimental uses of the WRF model for explicit severe-weather prediction in the United States (e.g. Done et al. 2004; Weisman et al. 2004; Kain et al. 2006). With "cold-start" initial conditions as well as boundary conditions supplied by the operational Eta model, these daily runs have involved grids with 4 km horizontal spacing, over computational domains that span more than two-thirds of the continental United States, and for time integrations of 24 to 36 hours. Of note here is the 4 km gridpoint spacing, which according to Weisman et al. (1997) is sufficiently small enough to resolve the evolution and key structural features of mesoscale convective systems, and hence seems to obviate the need for convective parameterization. These high-resolution WRF model predictions of convective storms – evaluated subjectively in terms of their initiation, evolution, and structure or mode – have compared well to observations on many, though certainly not all days (Kain et al. 2006). The conclusion seems to be that these high-resolution predictions have value.

Table 2. WRF model physics parameterization schemes.

Parameterization	**Name**
Microphysics Scheme	Lin et al. microphysics scheme
Radiation Schemes	Rapid Radiation Transfer Model longwave radiation scheme; Dudhia shortwave radiation scheme
Planetary Boundary Layer	Yonsei University PBL scheme
Convective Clouds and Precipitation	Kain-Fritsch cumulus parameterization scheme

b. The two approaches

The WFA utilizes the NNRP global dataset as initial and boundary conditions on the WRF model, which is then time-integrated for 30 h (hence the use of the "weather forecast" descriptor). The WFA employs three nested domains (hereinafter, d01, d02, d03) with 27 km, 9 km, and 3 km horizontal gridpoint spacing, respectively (Figs. 2 and 3); the vertical grid has 31 levels. Hence, the WRF is used as a regional (forecast) model that is then nested down to a convection-permitting domain (d03). Neither this domain nor d02 make use of a cumulus parameterization scheme; on the d01 domain, however, the Kain-Fritsch cumulus parameterization scheme is implemented. Two-way interaction between d03 and d02 is afforded, as it is between d02 and d01. The domains are judiciously placed according to location of event, sensitivity of the model to topography (i.e. mountains), and domain size (area large enough to analyze the event but small enough to be computationally efficient).

The RCMA uses the same NNRP global dataset to drive the RegCM3 model. The RegCM3 is run continuously over the domain shown in Figure 4 for more than one year (model time) prior to the historical events of interest here (i.e. 1 January 1973 – 5 April 1974, and 1 January 2000 – 10 May 2001). This allows for an equilibration between the modeled land surface processes and the overlying atmosphere (e.g., Giorgi and Mearns 1999); hence, the hypothesis is that the RegCM3 will add value to the modeling methodology by better representing the mesoscale circulations that are sensitive to or driven by soil moisture/temperature and their horizontal gradients. The RegCM3 output is then used as initial and boundary conditions on the WRF model, which is then time-integrated for 30 h.

For consistency with the WFA, the NNRP soil moisture and soil temperature, rather than that from the RegCM3, are used to initialize the WRF LSM. The three nested WRF domains remain the same for the RCMA as in the WFA. So, in the RCMA, the regional climate model drives the regional forecast model (d01), which is then nested down to a convection-permitting domain (d03).

It is important to mention here that the interaction between the RegCM3 and WRF is only one-way; similarly, the interaction between the NNRP and RegCM3 in the RCMA, and the NNRP and WRF in the WFA, is also one-way. This lack of feedback is acknowledged as a limitation. An effort at NCAR to develop a two-way nested regional climate model using the WRF and the Community Climate System Model (CCSM) will eventually remove this limitation[2].

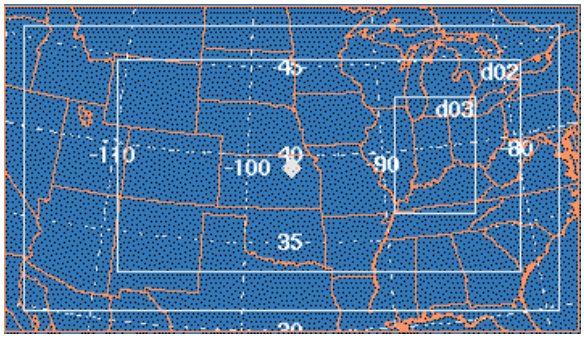

FIG 2. Computational domains for the WRF model used in the 3-4 April 1974 simulations. Domain 1 (d01) has a horizontal gridpoint spacing of 27 km, domain 2 (d02), of 9 km, and domain 3 (d03), of 3 km.

[2] For more information, see: http://www.mmm.ucar.edu/modeling/nrcm/index.php

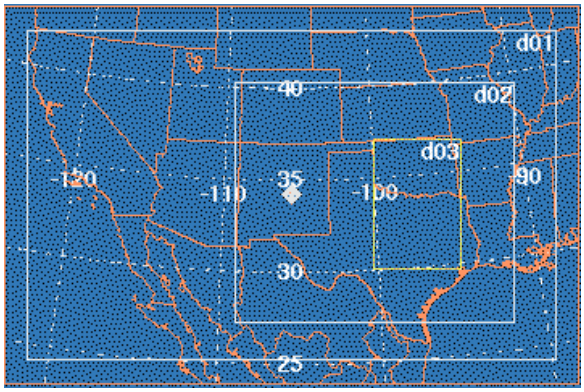

FIG 3. As in Figure 2 except for domains used in the 2-8 May 2001 simulations.

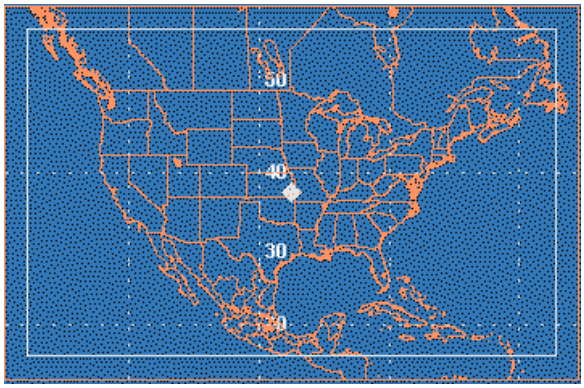

FIG 4. Computational domain for RegCM3.

3. WFA AND RCMA TESTING

a. Case studies

Two case studies are used to test the telescoping modeling approaches. The first is the Tornado Super Outbreak of 3-4 April 1974, considered to be one of the most devastating tornado outbreaks of the 20th century (Hoxit and Chappell 1975; Brooks and Doswell 2001). The second consists of the sequence of severe convective storms observed throughout the southern Great Plains during the period 2-8 May 2001. Well within the climatological peak for tornadoes and severe convective storms in Oklahoma and Texas (Concannon et al. 2000), this case is chosen to represent a "typical" occurrence of tornadoes and severe thunderstorms.

b. Assessment

In addition to a qualitative assessment of the model solutions, we seek an objective or quantitative means to compare model output to observations, and hence to evaluate the modeling approaches. Besides rain gauge data, the only relevant severe-storm observations (for the 1974 case, anyway) are reports of tornadoes, severe winds, and hail. Here, we choose tornado reports, because we hope to ultimately use one of the modeling approaches to generate climate statistics of tornadoes. Since we are not explicitly simulating tornado-scale motions, we require a model-based proxy of a tornado.

Consider the use of horizontal spatial correlations between vertical velocity and vertical vorticity as a means to identify supercells within model simulations (e.g. Davies-Jones 1984; Droegemeier et al. 1993). A form of this correlation, expressed as a *Supercell Detection Index*[3], was used during the 2005 SPC/NSSL Spring Program to locate possible supercells in high-resolution experimental forecasts. We have slightly adapted this index for our study, defining a parameter S at each gridpoint within domain d03 as

$$S = \left\langle \frac{w\zeta}{(w^2\zeta^2)^{1/2}} \right\rangle,$$

where w is vertical velocity, ζ is vertical vorticity, and the brackets $\langle\ \rangle$ indicate a *vertical* average, over each grid column, from the surface to approximately 5 km. To eliminate insignificant and/or spurious values, the w and ζ are required to surpass 5 m s^{-1} and 0.001 s^{-1} thresholds, respectively, at each grid level involved in the calculation.

Based on Droegemeier et al. (1993), Davies-Jones (1984), and the 2005 SPC/NSSL Spring Program, we assume here that $S > 0.6$ indicates a supercell and potential tornado. Specifically, each maxima (with $S > 0.6$) in the 2D field of S is used as a proxy for a tornado-producing supercell (e.g., Fig. 5), with the understanding that not all supercells or mesocyclonic storms spawn tornadoes (e.g. Trapp et al. 2005). Counts of maxima are determined over 1.5-h intervals[4], and then summed to arrive at a total number of assumed independent "tornado" detections over a 12-h period, within domain d03. These supercell-tornado proxies are then compared to the number of tornado reports over the same period and geographical domain.

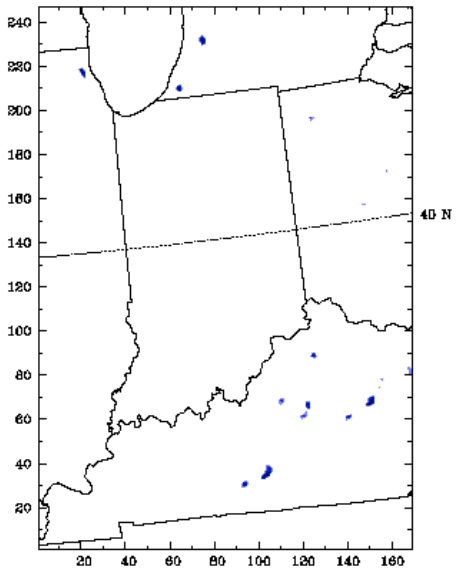

FIG 5. Evaluation of S, from the WFA solution at 0000 UTC 4 April 1974 on d03.

[3] See Attachment H, written by L. Wicker, J. Kain, S. Weiss, and D. Bright, in the 2005 SPC/NSSL Spring Program Overview and Operations Plan document by Weiss et al. (2005).

[4] Our experimentation shows that evaluation of S maxima over 1.5-h intervals should reveal independent supercells and thus tornado detections. This is consistent with the study by Burgess et al. (1982) who determined the core evolution of a mesocyclone to be 60 to 90 min.

c. Simulation results

The 30-h WRF simulations in both approaches and for both cases commence at 0000 UTC, which is roughly 12-15 h prior to convection initiation with d03. This initial ~12 h of simulation time is considered primarily to be the interval over which the model generates the mesoscale portion of the spectrum. Our discussion therefore focuses on the remaining part of the simulation, specifically on the evolution of the salient convective storm-scale features within d03. We then use the quantitative technique described above to compare the model output to observations. To be clear, we do not expect that specific storms of a given case will be simulated. Hence, in the assessments, time and especially space errors are acceptable as long as the simulations generate storms that are comparable in numbers, intensity, and convective mode.

(1) 3-4 April 1974

Weakly precipitating storms are found in d03 of the WFA solution by 1500 UTC on 3 April 1974 (hereinafter, the day and time are expressed following the convention 3/1500). As suggested in the radar summary charts presented by Hoxit and Chappell (1975), this early evolution in the WFA solution lags that of the observations by several hours. However, intense simulated storms with rotating updrafts are located in Indiana and Ohio by 3/2100 (Fig. 6a), consistent with the observed tornado reports as well as the Covington, Kentucky WSR-57 scans shown by Agee et al. (1975) (Fig. 7). Thereafter, simulated storms with supercell characteristics can be identified in eastern Illinois, Indiana, Ohio, and Kentucky through 4/0600, with 4/0000 as the time with the most numerous and intense convective storms (Fig. 6b).

The RCMA solution also lags the observations by several hours, with initiation of significant convective storms delayed until 3/2100 (Fig. 8). Some of these and other storms possessed supercell characteristics. The apparent supercell storms were never as numerous and widespread in the RCMA as in the WFA (and in the observations), as demonstrated next by the quantitative analysis.

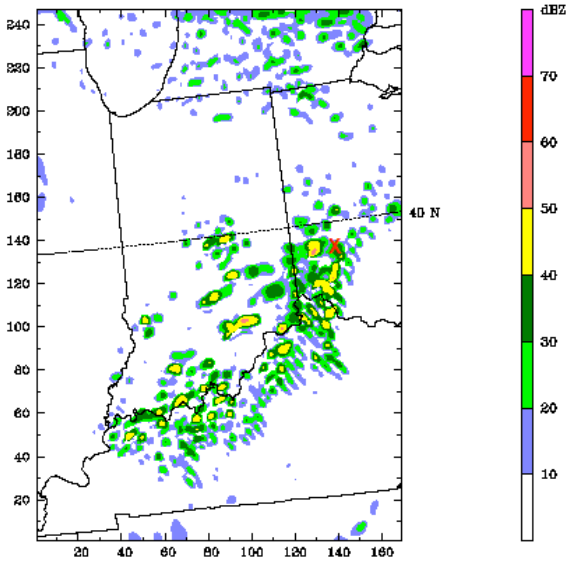

FIG 6a. WFA simulated reflectivity at 2100 UTC 3 April 1974 at 0.5 km AGL on d03. The "X" indicates approximate location of Xenia, Ohio.

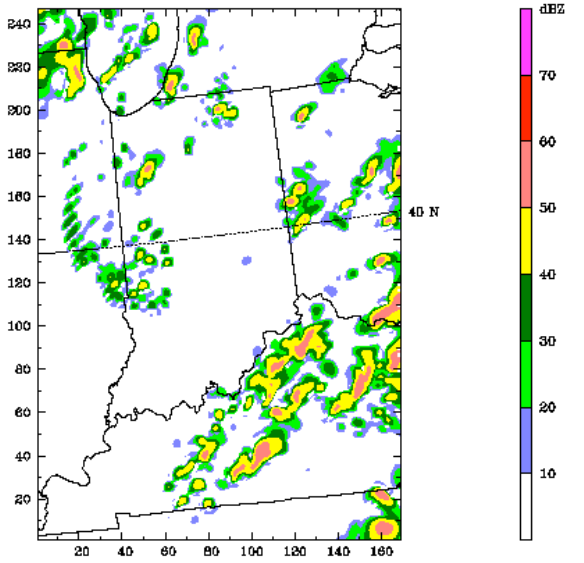

FIG 6b. WFA simulated reflectivity at 0000 UTC 4 April 1974 at 0.5 km AGL on d03.

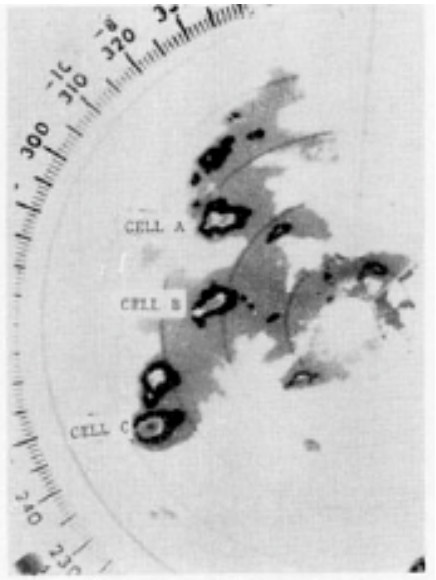

FIG 7. VIP display from the Covington, KY WSR-57, at 1947 UTC on 3 April 1974 (from Agee et al. 1975).

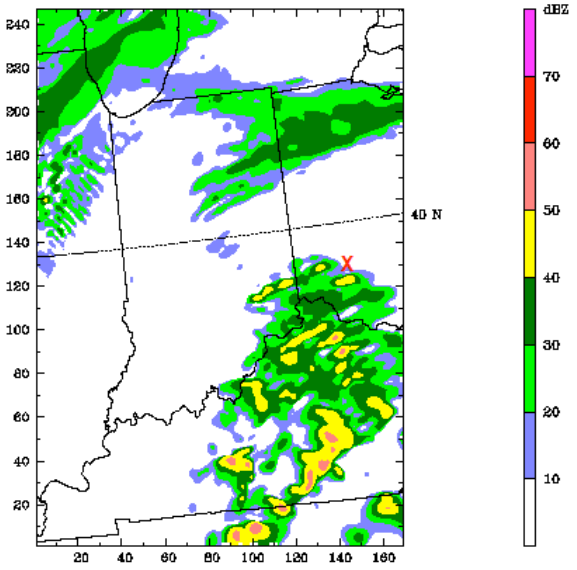

FIG 8a. RCMA simulated reflectivity at 2100 UTC 3 April 1974 at 0.5 km AGL on d03.

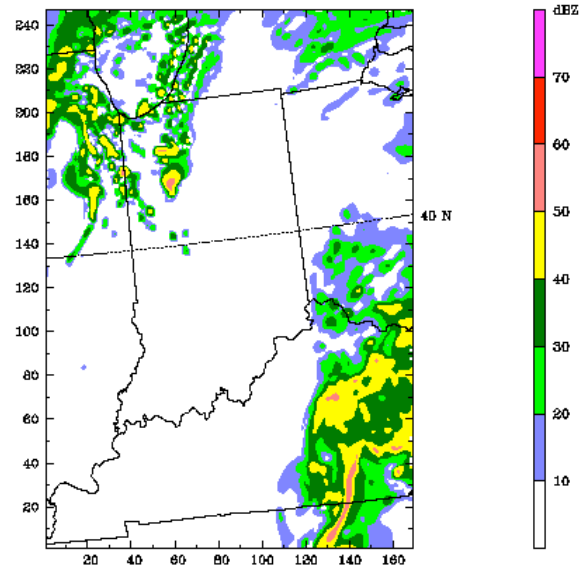

FIG 8b. RCMA simulated reflectivity at 0000 UTC 4 April 1974 at 0.5 km AGL on d03.

As summarized in Table 3, 64 supercell-tornado proxies or detections were determined from the WFA simulation over the period 3/1800 to 4/0600 and within domain d03. This number of detections compares quite well with the actual number of tornado reports (76), over the same period and geographical domain. In the spirit of the regional climate modeling "Big-Brother" experiments of Denis et al. (2002), additional WFA-type simulations were performed to examine solution sensitivity to: model spin-up time (model initialization at 2/1200), resolution ratio or "jump" (inclusion of an additional domain with 81-km grid spacing), and domain size and placement (extension of domain d01 to include the entire contiguous United States). Qualitatively, the solutions had differences in the details of individual storm characteristics and evolution (although not in convective mode). Quantitatively, however, they still resulted in comparatively high numbers of tornado detections (Table 3), which is most relevant to the goal of generating climate statistics of tornadoes.

In stark contrast to the WFA results, only 9 tornado detections were determined from the RCMA simulation (Table 4), owing simply to the relative lack of convective storms. Closer inspection of the RegCM3 output used as initial and boundary conditions revealed that, even though the synoptic-scale features (500 hPa trough axis, position of surface cyclone, etc.) were consistent with those in the WFA solution, the structure of the low-level thermodynamic fields was not. In particular, we found that the low-level air advected into Kentucky-Indiana-Ohio during the period 3/0000 to 3/1800 was relatively cool and dry, and consequently that the CAPE was small (less than ~100 J kg^{-1}). Further diagnosis revealed that the convective parameterization scheme in RegCM3 had activated in the vicinity of the southern boundary of the WRF domain (Fig. 9). In other words, air that had been cooled and stabilized was supplied to the WRF through its southern boundary condition.

To test this apparent sensitivity to the chance placement of the WRF d01 within the RegCM3 domain, experiments were conducted (i) with a much larger d01 that extended well into the Gulf of Mexico, and (ii) with the exclusion of the original d01, i.e., with only two nested domains (d02 and d03). Table 4 confirms the considerable sensitivity to the WRF domain placement, with both experiments resulting in an increase in the number of tornado detections by a factor of 3 to 4.

Table 3. Quantitative summary for WFA simulations of the 3-4 April 1974 case. The actual number of tornado reports over the period 3/1800 to 4/0600 and within the geographical domain described by d03 is 76.

Simulation Name	Tornado detections
WFA	64
Sensitivity: Spin Up Test	84
Sensitivity: Resolution Ratio Test	66
Sensitivity: Larger Domain Test	72

Table 4. As in Table 3 except for the RCMA.

Simulation Name	Tornado detections
RCMA	9
Sensitivity: 55km RCM Without d01	30
Sensitivity: Larger Domain d01	39

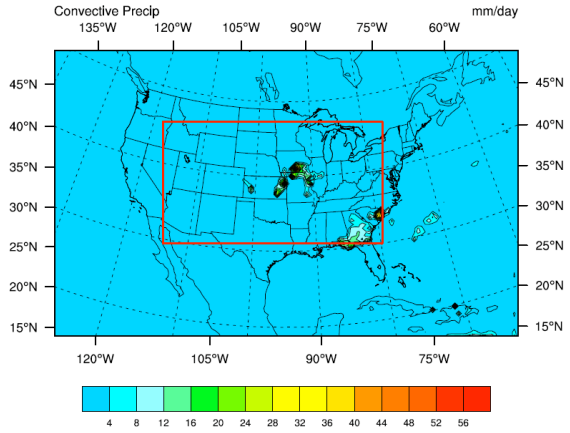

FIG 9. Convective precipitation (mm day^{-1}), from the RegCM3 simulation at 1800 UTC 3 Ap ril 1974. Approximate location of WRF domain d01 is outlined in red.

(2) 2-8 May 2001

During this convectively active week, tornadoes were reported (within d03) on 4, 5, and 6 May 2001. On the afternoon and evening of 4 May, an

extensive squall line was observed in Oklahoma through Texas (Fig. 10), with numerous incidents of severe weather and tornadoes reported in association with this line. The accuracy of the WFA solution on this day is open to question. Fig. 11 shows a line of cells extending from southwest Oklahoma to the southern Texas Panhandle, at 5/0000. Although this is not quite the same organization displayed in the radar composite, 6 tornado detections were found in d03 over the 12-h period 4/1800 to 5/0600, as compared to 11 tornado reports (Table 5).

On 5 May, isolated supercells as well as lines of convective storms were observed during the afternoon and evening (Fig. 12). The WFA was successful in simulating intense storms in Texas and Oklahoma on this day (Fig. 13), but produced too many with rotating updrafts in d03, as evidenced by the 44 tornado detections and the 3 tornado reports in d03 (Table 5). The WFA similarly overproduced tornado detections on 6 May and 7 May. The reason for this model behavior on these days is currently under investigation.

As with the previous case, the RCMA solutions for this case are dramatically different than the WFA solutions. In particular, the RCMA failed on all days during the period to generate intense, rotating storms and therefore tornado proxies. An explanation can be gained by examining the RegCM3 output that was used as initial and boundary conditions on the WRF model.

A significant synoptic-scale feature present in the observations (and in the NNRP data) near the beginning of the period was an upper-level cut-off low, centered in northeastern Arizona and southeastern Utah on 4/1200 (Fig. 14). Despite the fact that the RegCM3 was forced at its boundaries by the NNRP data, the model simulated at this time a progressive, small-amplitude trough rather than a cut-off low. The simple consequence of this error was a large-scale environment that could not support severe convection throughout the southern Great Plains.

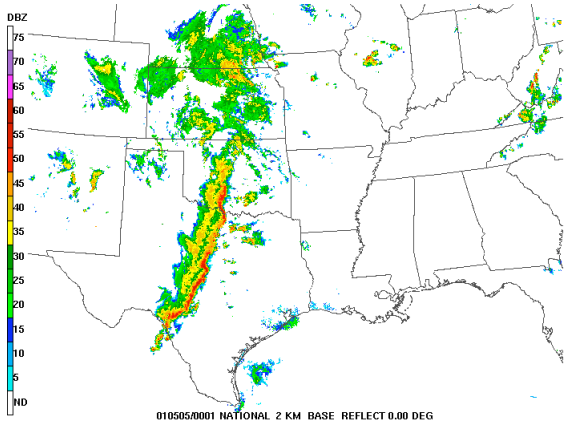

FIG 10. Composite base reflectivity at 0001 UTC 5 May 2001. (Image from the Storm Prediction Center)

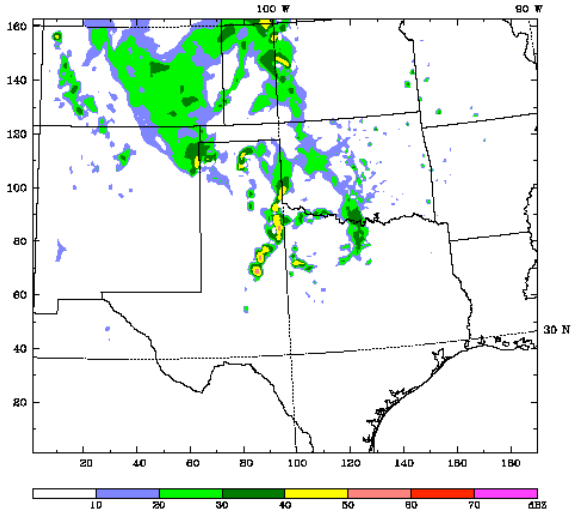

FIG 11. WFA simulated reflectivity at 0000 UTC 5 May 2001 at 0.5 km AGL on d02.

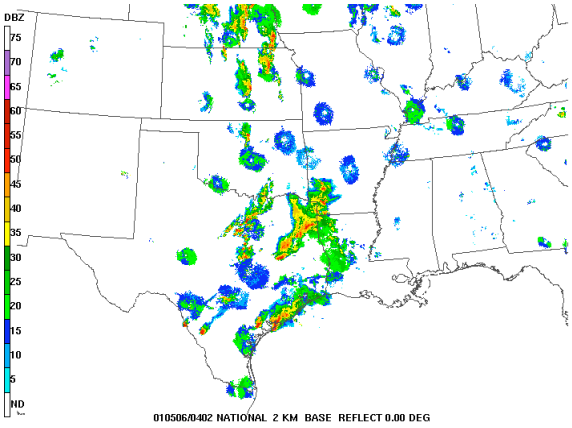

FIG 12. As in Fig. 10, except at 0402 UTC 6 May 2001.

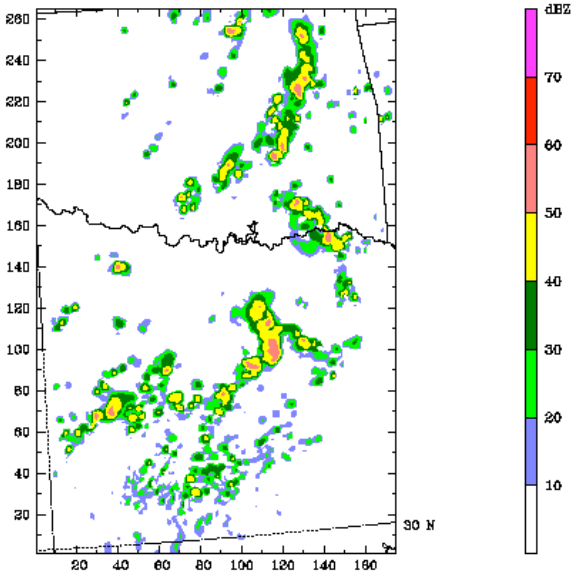

FIG 13. WFA simulated reflectivity at 0000 UTC 6 May 2001 at 0.5 km AGL on d03.

Table 5. Quantitative summary for daily WFA simulations over the period 2-8 May 2001. Note from the text that the RCMA failed generate any tornado detections during this period.

Simulation Name	Tornado detections	Actual Tornado Reports
2 May 2001	0	0
3 May 2001	5	0
4 May 2001	6	11
5 May 2001	44	3
6 May 2001	33	11
7 May 2001	46	0
8 May 2001	0	0

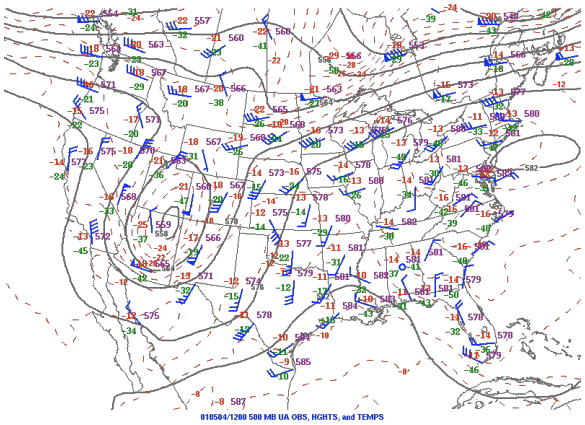

FIG 14. 1200 UTC 4 May 2001 500 hPa analysis. Station model plot, geopotential height contours (black) at 60 m intervals, and isotherms in 2ºC intervals. (Image from the Storm Prediction Center)

4. CONCLUDING REMARKS

Two telescoping modeling approaches were evaluated that could be used to investigate possible changes in the frequency, intensity, and geographical distribution of severe convective storms under future climate change. Both provide a means to dynamically

downscale global data. In the Regional Climate Modeling Approach (RCMA), a global dataset (or climate model) forces a regional climate model that in turn forces a convection permitting model that is nested, two-way interactively, within a regional forecast model. In the Weather Forecasting Approach (WFA), a global dataset (or climate model) directly forces the regional forecast model, within which a convection-permitting model is nested. The approaches were applied to two case studies.

Based on subjective and objective evaluations, the solutions from the WFA were superior to those from the RCMA. The RCMA's poor performance was due in one case to the large sensitivity of the placement of the WRF domain within the RegCM3, and in another case to the inaccurate simulation of the synoptic-scale flow.

We will subject these approaches to a final test before making any final conclusions. Specifically, we will use each to generate solutions over single or perhaps multiple-week periods, over multiple years. This will allow us to begin to compare, for example, model-based geographical tornado distributions to that based on tornado reports.

In addition to performing these longer-term, multiple realization tests, we have a number of other model issues that need to be addressed. These include, but are not limited to: (i) how to extract or generate compatible land-surface fields (e.g., soil moisture and temperature) from CAM and/or RegCM3 output that can be used to initialize the LSM in the WRF model; (ii) whether the use of multiple nests in the WRF model is acceptable for the current application, or if a single, ~contiguous U.S. domain at 3-4 km gridpoint spacing is necessary; and (iii) the reliability and sensitivity of the tornado proxy technique, and how to use this technique to construct proxy-based geographical distributions.

ACKNOWLEDGEMENTS

This work exemplifies research under the Climate and Extreme Weather initiative within the Department of Earth and Atmospheric Sciences at Purdue University, and was supported in part by NSF ATM-0541491.

REFERENCES

Agee, E., C. Church, C. Morris, and J. Snow, 1975: Some synoptic aspects and dynamic features of vortices associated with the tornado outbreak of 3 April 1974, *Mon. Wea. Rev.*, **103**, 318-333.

Bell, J. A., L.C. Sloan, and M.A. Snyder, 2004: Regional changes in extreme climatic events: A future climate scenario, *J. Climate*, **17**, 81-87.

Brooks, H.E., 2005: A global view of severe thunderstorms: Estimating the current distribution and possible future changes, *Preprints*, Symposium on the Challenges of Severe Convective Storms, Atlanta, GA, American Meteorological Society, **J4.2**.

Brooks, H. E. and C.A. Doswell: 2001: Normalized damage from major tornadoes in the United States: 1890-1999, *Wea. Forecasting*, **16**, 168-176.

Brown, B.G. and R.W. Katz, 1995: Regional analysis of temperature extremes: Spatial analog for climate change, *J. Climate*, **8**, 108-119.

Burgess, D.W., V. T. Wood, and R. A. Brown, 1982: Mesocyclone evolution statistics, Preprints, *12th Conf. on Severe Local Storms,* San Antonio, TX, Amer. Meteor. Soc., 422–424.

Carnell, R.E., and C.A. Senior, 1998: Changes in mid-latitude variability due to increasing greenhouse gases and sulphate aerosols, *Clim. Dyn.*, **14**, 369-383.

Concannon, P.R., H.E. Brooks, and C.A. Doswell III, 2000: Climatological risk of strong and violent tornadoes in the United States, *2nd Conference on Environmental Applications*, **P 9.4**.

Davies-Jones, R. P., 1984: Streamwise vorticity: The origin of updraft rotation in supercell storms, *J. Atmos. Sci.*, **41**, 2991-3006.

Denis, B., R. Laprise, D. Caya, and J. Côté, 2002: Downscaling ability of one-way nested regional climate models: The Big-Brother Experiment, *Climate Dyn.*, **18**, 627-646.

Diffenbaugh, N. S., J. S. Pal, R. J. Trapp, and F. Giorgi, 2005: Interactions of large- and fine-scale processes dictate the greenhouse response of extreme daily climate events over the United States. *Proceedings, National Academy of Sciences*, 102, 15774-15778.

Doswell, C.A.III and D.W. Burgess, 1993: Tornadoes and tornadic storms: A review of conceptual models, *The Tornado: Its Structure, Dynamics, Prediction, and Hazards* (Church et al, eds). Amer. Geophys. Uniton, Geophys. Monogr., **79**, 161-172.

Droegemeier, K. K., S. M. Lazarus, and R. P. Davies-Jones, 1993: The influence of helicity on numerically simulated convective storms, *Mon. Wea. Rev.*, **121**, 2005-2029.

Dudhia, J., 1989: Numerical study of convection observed during the winter monsoon experiment using a mesoscale two-dimensional model, *J. Atmos. Sci.*, **46**, 3077-3107.

Giorgi, F., 1990: Simulation of regional climate using a limited area model nested in a general circulation model, *J. Climate*, **3**, 941-963.

Giorgi, F., G. Bates, and S. Nieman, 1993a: The multi-year surface climatology of a regional atmospheric model over the western United States, *J. Climate*, **6**, 75-95.

Giorgi, F., and L. O. Mearns, 1999: Introduction to special section: Regional climate modeling revisited, *J. Geophy. Res.*, **104**, no. D6, 6335-6352.

Giorgi, F., X. Bi, and J.S. Pal, 2004: Mean, interannual variability and trends in a regional climate experiment over Europe. I: Present day climate, *Clim. Dyn.,* **22**, 733-756.

Hoxit, L.R. and C.F. Chappell, 1975: Tornado outbreak of April 3-4, 1974: Synoptic analysis, *NOAA Tech. Report*, Boulder, CO.

IPCC, 2001: Climate Change 2001: The Scientific Basis. Contribution of Working Group I to the Third Assessment Report of the Intergovernmental Panel on Climate Change (IPCC). [J. T. Houghton, Y. Ding, D.J. Griggs, M. Noguer, P. J. van der Linden and D. Xiaosu (Eds.)], Cambridge University Press, UK, 944 pp.

Kalnay, E., M. Kanamitsu, R. Kistler, W. Collins, D. Deaven, L. Gandin, M. Iredell, S. Saha, G. White, J. Woollen, Y. Zhu, M. Chelliah, W. Ebisuzaki, W. Higgins, J. Janowiak, K.C. Mo, C. Ropelewski, J. Wang, A. Leetmaa, R. Reynolds, R. Jenne, and D. Joseph, 1996: The NCEP/NCAR 40-Year reanalysis project, *Bull. Amer. Met. Soc.*, **77**, 437-471.

Kain, J.S., S.J. Weiss, J.J. Levit, M.E. Baldwin, and D.R. Bright, 2006: Examination of convection-allowing configurations of the WRF model for the prediction of severe convective weather: The SPC/NSSL spring program 2004, *Wea. Forecasting*, **21**, 167-181.

Lilly, D.K., 1979: The dynamical structure and evolution of thunderstorms and squall lines, *Ann. Rev. Earth Planet. Sci.*, **7**, 117-171.

Lin, Y.-L., R.D. Farley, and H.D. Orville, 1983: Bulk parameterization of the snow field in a cloud model, *J. Clim. Appl. Meteor.*, **22**, 1065-1092.

Michalakes, J., S. Chen, J. Dudhia, L. Hart, J. Klemp, J. Middlecoff, and W. Skamarock, 2001: Development of a next generation regional weather research and forecast model *Developments in Teracomputing*: *Proceedings of the Ninth ECMWF Workshop on the Use of High Performance Computing in Meteorology*, Eds. Walter Zwieflhofer and Norbert Kreitz, World Scientific, Singapore, 269-276.

Pal, J., E. Small, and E. Eltahir, 2000: Simulation of regional-scale water and energy budgets: Representation of subgrid cloud and precipitation processes within RegCM, *J. Geophy. Res.-Atmos.*, 105(D24), 29579-29594.

Pal, J.S., F. Giorgi, and X. Bi, 2004: Consistency of recent European summer precipitation trends and extremes with future regional climate projections, *Geophy. Res. Let.*, **31**, L13202.

Skamarock, W.C., J.B. Klemp, J. Dudhia, D.O. Gill, D.M. Barker, W. Wang and J.G. Powers, 2005: A description of the Advanced Research WRF Version 2, NCAR Tech Note, NCAR/TN-468+STR, 88 pp.

Trapp, R. J., G. J. Stumpf, and K. L. Manross, 2005: A reassessment of the percentage of tornadic mesocyclones. *Wea. Forecasting*, **20**, 680-687.

Weisman, M. L., C. Davis, J. Done, W. Wang, and J. Bresch, 2004: Real-time explicit convective forecasts using the WRF model during the BAMEX field program, *20th Conference on Weather Analysis and Forecasting/16th Conference on Numerical Weather Prediction*, January 10-15, 2004.

Weisman, M.L, W.C. Skamarock, and J.B. Klemp, 1997: The resolution dependence of explicitly modeled convective systems, *Mon. Wea. Rev.,* **125**, 527-548.

Weiss, S., J. Kain, J. Levit, M. Baldwin, D. Bright, G. Carbin, and J. Hart, 2005: SPC/NSSL Spring program 2005: Program overview and operations plan.